

ON SOME NONLOCAL MODELS WITH RADially SYMMETRIC INTERACTION DOMAINS AND THE EFFECT OF DOMAIN TRUNCATION

QIANG DU*, HEHU XIE†, AND XIAOBO YIN‡

Abstract. Many nonlocal models have adopted a finite and radially symmetric nonlocal interaction domains. When solving them numerically, it is sometimes convenient to adopt polygonal approximations of such interaction domains. A crucial question is, to what extent such approximations affect the nonlocal operators and the corresponding nonlocal solutions. While recent works have analyzed this issue for nonlocal operators in the case of a fixed horizon parameter, the question remains open in the case of a small or vanishing horizon parameter, which happens often in many practical applications and has significant impact on the reliability and robustness of nonlocal modeling and simulations. In this work, we are interested in addressing this issue and establishing the convergence of new nonlocal solutions by polygonal approximations to the local limit of the original nonlocal solutions. Our finding reveals that the new nonlocal solution does not converge to the correct local limit when the number of sides of polygons is uniformly bounded. On the other hand, if the number of sides tends to infinity, the desired convergence can be shown. These results may be used to guide future computational studies of nonlocal problems.

Key words. Nonlocal models, peridynamics, polygonal approximation, horizon parameter, asymptotically compatible, convergence

AMS subject classifications. 45A05, 45N05, 45P05, 46N20, 65R20, 65R99

1. Introduction. Nonlocal models that account for interaction occurring at a distance have been shown to provide improved simulation fidelity in the presence of long-range forces and anomalous behaviors [11]. For this reason, they have found interesting applications in a variety of research fields such as fracture mechanics [21, 26, 36], phase transitions [1, 7, 18], stochastic processes [5, 9, 28, 32] and image processing [4, 19, 20, 27].

There has been much recent interest in developing numerical algorithms for nonlocal models [8], including finite difference [14, 39, 41], finite element [16, 41, 49], collocation [40, 46, 50] and meshfree [22, 24, 25, 37] methods. For mesh dependent numerical schemes in high dimensional cases, like finite difference and finite element methods, the meshes are often composed of polygons or polyhedra. On the other hand, the nonlocal interaction regions are ubiquitously chosen to be Euclidean balls, leading to the challenge of dealing with intersections of such balls with the polygonal or polyhedral elements. To mitigate the challenge, polygonal or polyhedral approximation of balls has been presented as a possible option [10, 45]. For mesh-free schemes, one also needs to take care of the numerical treatment of nonlocal interaction regions properly, often involving the implementation of various volume correction strategies,

*Department of Applied Physics and Applied Mathematics, Columbia University, NY 10027, USA (qd2125@columbia.edu). The research of this author is supported in part by National Science Foundation grants DMS-2012562 and DMS-1937254.

†LSEC, ICMSEC, Academy of Mathematics and Systems Science, Chinese Academy of Sciences, Beijing 100190, China, and School of Mathematical Sciences, University of Chinese Academy of Sciences, Beijing, 100049, China (hxie@lsec.cc.ac.cn). The research of this author is supported by the National Natural Science Foundations of China 11771434, Beijing Natural Science Foundation Z200003 and the National Center for Mathematics and Interdisciplinary Science, CAS.

‡School of Mathematics and Statistics & Hubei Key Laboratory of Mathematical Sciences, Central China Normal University, Wuhan 430079, China (yinxbo@mail.ccn.edu.cn). The research of this author is supported by the National Natural Science Foundation of China 11671165 and Hubei Provincial Science and Technology Innovation Base (Platform) Special Project 2020DFH002.

see [33, 51]. A natural question is, to what extent such approximations affect the nonlocal operators and the corresponding nonlocal solutions. In particular, an important aspect of this question is how such approximations may affect the consistency with well-known local limits of the nonlocal models, should such limits make sense. This is the issue that we focus on in the current work since it may have a significant impact on the reliability and robustness of nonlocal modeling and simulations.

We can reformulate the issue in terms of the diagram shown in Figure 1, which also summarizes the existing literature and the main contributions of this work. We use \mathcal{L}_δ to represent a nonlocal operator with the horizon parameter δ measuring the radius of the radially symmetric nonlocal interaction domain. Meanwhile, $\mathcal{L}_{\delta, n_\delta}$ is used to represent a nonlocal operator obtained from \mathcal{L}_δ by replacing the radially symmetric nonlocal interaction domain with a suitable polygonal approximation. The integer n_δ denotes the maximum numbers of sides of the polygons (or faces for polyhedra), and we use $n_\delta = \infty$ to represent the case that the polygonal/polyhedral domain with infinite number of sides recovers the radially symmetric domain. \mathcal{L}_0 denotes the local limit of \mathcal{L}_δ as $\delta \rightarrow 0$. The nonlocal problem is stated as $-\mathcal{L}_\delta u_\delta = f_\delta$ with f_δ denoting prescribed data and u_δ denoting the nonlocal solution. Similarly, we have the corresponding nonlocal problem $-\mathcal{L}_{\delta, n_\delta} u_{\delta, n_\delta} = f_\delta$ and local problem $-\mathcal{L}_0 u_0 = f$ with f be the limit of f_δ as $\delta \rightarrow 0$ in L^2 sense, respectively. The dashed and dotted arrows are the main directions studied in this paper, while the solid ones stand for cases previously investigated in the literature. In particular, the dashed line, marked with $\not\rightarrow$ signs, indicates a path that the nonlocal solution u_{δ, n_δ} fails to converge to the correct local solution u_0 if n_δ remains bounded as $\delta \rightarrow 0$. This result can be found later in subsection 3.2 where we show that for a generic quadratic function $q = q(\mathbf{x})$, $\mathcal{L}_{\delta, n_\delta} q$ will not converge to $\mathcal{L}_0 q$ if n_δ has a uniform upper bound as $\delta \rightarrow 0$. On the other hand, the dotted line corresponds to a path that u_{δ, n_δ} converges to u_0 if n_δ tends to infinity as $\delta \rightarrow 0$. This can be found in subsection 3.3 where we derive three sufficient conditions to ensure the convergence of u_{δ, n_δ} to u_0 .

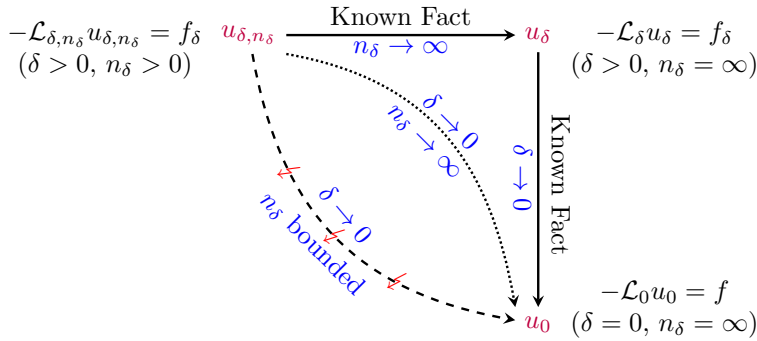


FIG. 1. A convergence diagram representing nonlocal problems with different nonlocal interaction domains and their local limits

The convergence diagram in Figure 1 is reminiscent to [42, Figure 1] (see also [43, Figure 2.1]) where the concept of Asymptotically Compatible (AC) schemes is formally proposed to study the convergence of numerical approximations to nonlocal problems and their local limits. One may find a number of recent studies on various AC schemes for nonlocal models, see for example [14, 23, 24, 48, 44, 50] and additional references cited therein. While the diagram in Figure 1 can be regarded

as a discussion on some kind of AC property, its implications are different. In fact, although motivated by numerical discretizations, the diagram in [Figure 1](#) does not have to involve any numerical schemes. Instead, one may interpret the diagram completely on the continuum level and the main focus is on the effect of the polygonal or polyhedral approximations to the nonlocal operators. Nevertheless, the findings given by the diagram shed light on the potential risks involved in simulations of nonlocal problems with different interaction domains. They provide theoretical guidance to the design and analysis of numerical algorithms when truncations of nonlocal interaction domains are adopted.

More precise statements and rigorous derivations of the findings shown in [Figure 1](#) are given later in [section 3](#). In preparation, we present detailed descriptions on the nonlocal operators \mathcal{L}_δ and $\mathcal{L}_{\delta, n_\delta}$ and the local limit \mathcal{L}_0 , as well as some review of related literature in [section 2](#). In particular, the convergence of u_δ to u_0 is reviewed. For illustration, we choose to work with the two dimensional case, while extension to higher dimensional cases is discussed in [subsection 3.5](#). We also provide some examples of popular nonlocal operators in [subsection 3.4](#) to illustrate that our theory is widely applicable. Results of numerical experiments are reported in [section 4](#) to validate the theoretical studies. Finally, we give some conclusions in [section 5](#).

2. Background and notation. Let $\Omega \subset \mathbb{R}^d$ denote a bounded, open and convex domain. For $u(\mathbf{x}) : \Omega \rightarrow \mathbb{R}$, the nonlocal operator \mathcal{L}_δ acting on $u_\delta(\mathbf{x})$ is defined as

$$(2.1) \quad \mathcal{L}_\delta u(\mathbf{x}) = 2 \int_{\mathbb{R}^d} (u(\mathbf{y}) - u(\mathbf{x})) \gamma_\delta(\mathbf{x}, \mathbf{y}) d\mathbf{y} \quad \forall \mathbf{x} \in \Omega,$$

where the nonnegative symmetric mapping $\gamma_\delta(\mathbf{x}, \mathbf{y}) : \mathbb{R}^d \times \mathbb{R}^d \rightarrow \mathbb{R}$ is called a kernel function. In general, the integral in [\(2.1\)](#) is understood in the principal value sense. In this paper, we consider the following nonlocal homogeneous Dirichlet volume-constrained diffusion problem

$$(2.2) \quad \begin{cases} -\mathcal{L}_\delta u_\delta(\mathbf{x}) &= f_\delta(\mathbf{x}) & \text{on } \Omega, \\ u_\delta(\mathbf{x}) &= 0 & \text{on } \Omega_\delta^c, \end{cases}$$

where Ω_δ^c denotes the interaction domain corresponding to Ω , $f_\delta(\mathbf{x}) \in L^2(\Omega)$ is a given function depending on δ . Here we use homogeneous Dirichlet boundary condition to avoid the impact from boundary condition. Readers who are interested in the convergence behavior for nonlocal solutions to their local limits under different kinds of nonlocal boundary conditions are referred to [\[6, 17, 38, 47, 48\]](#). For convenience we denote by $\widehat{\Omega}_\delta = \Omega \cup \Omega_\delta^c$.

2.1. Radially symmetric nonlocal interaction kernels with finite interaction radius. In this work, we are interested in problems where the interactions occur over finite distances. The kernels are thus assumed to have bounded support, i.e., $\gamma_\delta(\mathbf{x}, \mathbf{y}) \neq 0$ only if \mathbf{y} is within a bounded neighborhood of \mathbf{x} . For this neighborhood, we discuss the choice of Euclidean balls $B_\delta(\mathbf{x})$ centered at \mathbf{x} with radius δ , i.e.,

$$(2.3) \quad \forall \mathbf{x} \in \Omega : \gamma_\delta(\mathbf{x}, \mathbf{y}) = 0, \quad \forall \mathbf{y} \in \mathbb{R}^d \setminus B_\delta(\mathbf{x}),$$

while δ is known as the horizon parameter or interaction radius. Under this condition, the interaction domain is defined as $\Omega_\delta^c = \{\mathbf{y} \in \mathbb{R}^d \setminus \Omega : \text{dist}(\mathbf{y}, \partial\Omega) < \delta\}$. Besides [\(2.3\)](#), the kernel function $\gamma_\delta(\mathbf{x}, \mathbf{y})$ is assumed to satisfy the following conditions:

$$(2.4) \quad \gamma_\delta(\mathbf{x}, \mathbf{y}) = \widetilde{\gamma}_\delta(|\mathbf{y} - \mathbf{x}|) > 0 \text{ for } |\mathbf{y} - \mathbf{x}| < \delta, \text{ and } \int_{B_\delta(\mathbf{0})} |\mathbf{z}|^2 \widetilde{\gamma}_\delta(|\mathbf{z}|) d\mathbf{z} = d.$$

Note that the first condition means that the kernel is strictly positive for \mathbf{y} inside $B_\delta(\mathbf{x})$. The second condition of (2.4) is set to ensure that if the operator \mathcal{L}_δ converges to a limit as $\delta \rightarrow 0$, then the limit is given by $\mathcal{L}_0 = \Delta$, the classical diffusion operator, see related materials and discussions in [42, 43]. Assuming further that $f_\delta \rightarrow f_0$ in $L^2(\Omega)$ as $\delta \rightarrow 0$, the corresponding local problem is defined as follows:

$$(2.5) \quad \begin{cases} -\mathcal{L}_0 u_0(\mathbf{x}) = f_0(\mathbf{x}) & \text{on } \Omega, \\ u_0(\mathbf{x}) = 0 & \text{on } \partial\Omega. \end{cases}$$

This means that as $\delta \rightarrow 0$, the nonlocal effect diminishes and nonlocal equations converge to a classical local differential equation. Such limiting behavior reflects connections and consistencies between nonlocal and local models and has great practical significance especially for multiscale modeling and simulations.

To make the analysis later more concise, we further assume that $\gamma_\delta(\mathbf{x}, \mathbf{y})$ is a rescaled translation-invariant kernel function, that is,

$$(2.6) \quad \gamma_\delta(\mathbf{x}, \mathbf{y}) = \frac{1}{\delta^{d+2}} \gamma\left(\frac{|\mathbf{y} - \mathbf{x}|}{\delta}\right)$$

for some kernel function $\gamma(|\cdot|)$ that is assumed to be radial, nonnegative, compactly supported in $B_1(\mathbf{0})$, and has a bounded second-order moment, that is,

$$|\xi|^2 \gamma(|\xi|) \in L^1_{\text{loc}}(\mathbb{R}^d) \quad \text{and} \quad \int_{B_1(\mathbf{0})} |\xi|^2 \gamma(|\xi|) d\xi = d.$$

By (2.3) and (2.4), we see that the support set of γ is $B_1(\mathbf{0})$, thus, for any subdomain $D_s \subset B_1(\mathbf{0})$ of nonzero measure, that is, $|D_s| > 0$, we have

$$(2.7) \quad \int_{D_s} |\xi|^2 \gamma(|\xi|) d\xi > 0.$$

2.2. Motivation for nonlocal models with different interaction domains.

When solving nonlocal problems like (2.2) on computers using mesh based numerical methods such as finite element approximations, a popular strategy is to use various polygonal approximations of Euclidean balls [10, 45]. This helps to eliminate the complications to handle nonlocal interactions at the ball-element intersections. A natural question is, to what extent the precision is affected when contributions from some of these spherical caps (abbreviated as caps) are thrown away or approximated by some triangles. One can find in [10, 45] discussions on how the resulted approximations, in combination with quadrature rules, affect the discretization error, including the estimate on the convergence rate with respect to the mesh size h between the original continuous linear finite element solution (denoted by u_δ^h) associated with the exact Euclidean ball and that (denoted by $u_{\delta, n_\delta}^{h, \#}$) associated with ‘approximate balls’ $B_{\delta, n_\delta}^\#$ (polygons/polyhedra with n_δ being the number of sides/faces). Using suitably modified notation and descriptions, we review these known convergence result as follows.

PROPOSITION 2.1. [10, Corollary 4.2] *Assume that the kernel function is square integrable (or integrable and translationally invariant) and bounded for all $B_\delta(\mathbf{x}) \ominus B_{\delta, n_\delta}^\#(\mathbf{x})$ (which denotes the symmetric difference between $B_\delta(\mathbf{x})$ and $B_{\delta, n_\delta}^\#(\mathbf{x})$). Then,*

$$(2.8) \quad \left\| u_\delta^h - u_{\delta, n_\delta}^{h, \#} \right\|_{L^2} \leq CK \sup_{\mathbf{x} \in \Omega} \left| B_\delta(\mathbf{x}) \ominus B_{\delta, n_\delta}^\#(\mathbf{x}) \right|,$$

where \sharp represents one of the following possible choices

$$(2.9) \quad \{\text{regular, nocaps, approxcaps, 3vertices, 123vertices, 23vertices, barycenter}\}.$$

Here $B_{\delta, n_\delta}^{\text{regular}}(\mathbf{x})$ is an n_δ -sided inscribed regular polygon of $B_\delta(\mathbf{x})$, while $B_{\delta, n_\delta}^{\text{nocaps}}(\mathbf{x})$ stands for the polygon generated by throwing away all caps formed whenever the circular boundary of the ball $B_\delta(\mathbf{x})$ intersects the sides of a triangle. The caps are approximated by sub-triangles which, together with $B_{\delta, n_\delta}^{\text{nocaps}}(\mathbf{x})$, results to $B_{\delta, n_\delta}^{\text{approxcaps}}(\mathbf{x})$.

$B_{\delta, n_\delta}^\sharp(\mathbf{x})$ with $\sharp \in \{\text{3vertices, 123vertices, 23vertices, barycenter}\}$ stands for the cases that ‘three vertices’, ‘at least one vertex’, ‘at least two vertices’, ‘triangle barycenters’ are inside the ball, respectively. These seven types of polygonal approximations are depicted in Figure 2. For a more detailed description, please refer to [10].

Then based on the geometric estimate

$$\left| B_\delta(\mathbf{x}) \ominus B_{\delta, n_\delta}^\sharp(\mathbf{x}) \right| = \mathcal{O}(h^\alpha), \text{ with } \alpha \in [1, 2],$$

it was shown that

$$(2.10) \quad \left\| u_\delta^h - u_{\delta, n_\delta}^{h, \sharp} \right\|_{L^2} \sim \mathcal{O}(h^\alpha),$$

when the continuous linear finite element approximations are used, for which the rate of convergence is $\mathcal{O}(h^2)$ at best. For example, with $\sharp = \text{nocaps}$, we have $\alpha = 2$. While the existing convergence results are encouraging, we note that the result (2.8)

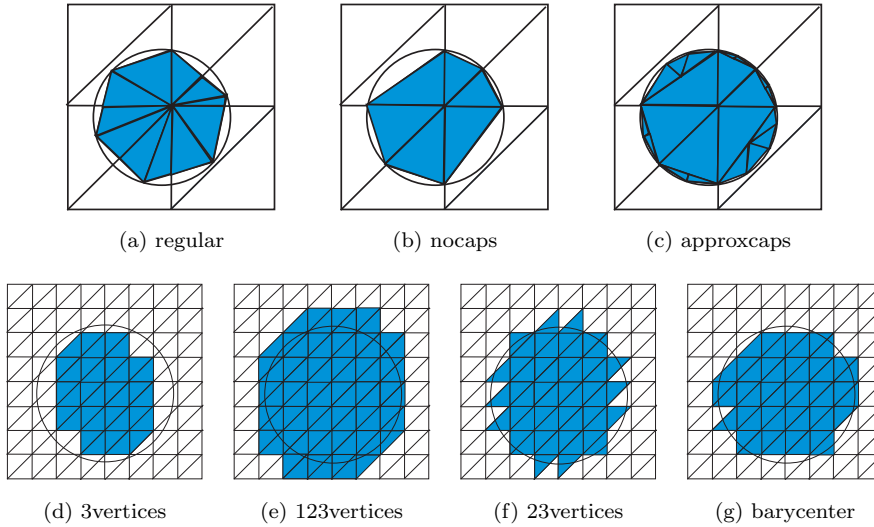


FIG. 2. Polygonal approximate balls

is derived by ignoring the dependence on the parameter δ . After a careful examination of the assumption on the kernel function for achieving (2.8) and the detailed proof in [10], we find that (2.8) holds only for a fixed δ . In fact, to reflect the dependence on δ , K needs to be modified as $K(\gamma_\delta)$, which is defined by

$$(2.11) \quad K(\gamma_\delta) = \sup_{\mathbf{x} \in \Omega} \left(\int_{(B_\delta(\mathbf{x}) \ominus B_{\delta, n_\delta}^\sharp(\mathbf{x})) \cap \hat{\Omega}_\delta} \gamma_\delta(\mathbf{x}, \mathbf{y}) d\mathbf{y} \right).$$

For the constant kernel function considered in [10, Section 8], that is

$$(2.12) \quad \gamma(t) = \frac{4}{\pi}, \text{ for } 0 < t \leq 1,$$

we have $K(\gamma_\delta) \sim \mathcal{O}(\delta^{-4})$. Thus (2.10) becomes

$$(2.13) \quad \left\| u_\delta^h - u_{\delta, n_\delta}^{h, \#} \right\|_{L^2} \sim \mathcal{O}(\delta^{-4} h^\alpha), \text{ with } \alpha \in [1, 2],$$

which means that one may not always expect the convergence for any pair of (δ, h) as $\delta \rightarrow 0$ and $h \rightarrow 0$. As suggested in [37], the ratio $\delta/h = 3$ is usually adopted in practice for macroscale modeling by peridynamics model which is a popular class of nonlocal models. With this choice of the the horizon parameter and mesh parameter, the convergence likely might not hold according to (2.13). This motivates the current study. However, to avoid the complications, we choose to first examine the effect of truncation of interaction domains on the nonlocal operators on the continuum level in this work, while leaving the study that also accounts for the numerical discretization to subsequent investigations. Indeed, our approach can also be adopted in the discrete setting so that similar results can also be established for mesh based numerical approximations. For example, if continuous linear finite element method is used, the question raised earlier could be answered afresh: for all types of polygonal approximations of Euclidean balls listed in (2.9), if the ratio δ/h is uniformly bounded, $\left\| u_\delta^h - u_{\delta, n_\delta}^{h, \#} \right\|_{L^2}$ does not converge to zero as $\delta \rightarrow 0$. The corresponding numerical analysis is presented thoroughly in the companion article [15] where it is shown that the estimate (2.8) with K replaced by $K(\gamma_\delta)$ is too conservative. In fact, in comparison with the result (2.13), one may establish a *conditional* convergence rate of the form

$$(2.14) \quad \left\| u_\delta^h - u_{\delta, n_\delta}^{h, \#} \right\|_{L^2} \leq C (h^2 \delta^{-2} + h^2 \delta^{-1}).$$

Here, conditional convergence means that the error only diminish subject to the condition $h/\delta \rightarrow 0$ as both $\delta \rightarrow 0$ and $h \rightarrow 0$. Our study here provides hints to the necessity of this condition. For more detailed derivations on such convergence results, we refer to [15], which is a further study built upon the results of this paper.

2.3. Nonlocal operators with truncated polygonal/polyhedral interaction domains. In this paper, we aim to study the convergence property for a series of continuum nonlocal operators $\mathcal{L}_{\delta, n_\delta}$ as $\delta \rightarrow 0$, which depends on a family of polygons or polyhedra that approaches to the spherical interaction balls.

As in [12] the nonlocal energy norm and nonlocal volume constrained energy space are defined by

$$\|u\|_\delta := \left(\int_{\widehat{\Omega}_\delta} \int_{\widehat{\Omega}_\delta} (u(\mathbf{y}) - u(\mathbf{x}))^2 \gamma_\delta(\mathbf{x}, \mathbf{y}) d\mathbf{y} d\mathbf{x} \right)^{1/2},$$

and

$$V(\widehat{\Omega}_\delta) := \left\{ u \in L^2(\widehat{\Omega}_\delta) : \|u\|_\delta < \infty, u(\mathbf{x}) = 0 \text{ on } \Omega_\delta^c \right\},$$

respectively.

For the sake of simple illustration, we present the following discussion in two dimensional case and proceed in such a setting for the remainder of the convergence study, while extension to higher dimensional cases is discussed in subsection 3.5.

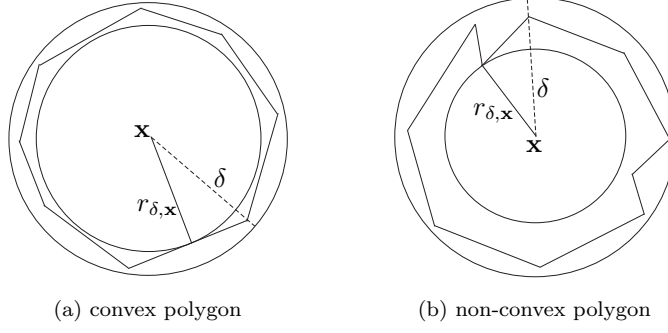


FIG. 3. Polygons in the circle $B_\delta(\mathbf{x})$

For any $\mathbf{x} \in \Omega$, a polygon inside the circle $B_\delta(\mathbf{x})$ is denoted by $B_{\delta, n_\delta, \mathbf{x}}(\mathbf{x})$, or simply $B_{\delta, n_\delta, \mathbf{x}}$, where n_δ, \mathbf{x} denotes the number of sides. Furthermore, to make use of (2.6), the rescaled polygon of $B_{\delta, n_\delta, \mathbf{x}}$ is define as

$$(2.15) \quad B_{1, n_\delta, \mathbf{x}}(\mathbf{0}) = \{ \mathbf{z} = (\mathbf{y} - \mathbf{x}) / \delta : \mathbf{y} \in B_{\delta, n_\delta, \mathbf{x}} \}.$$

For a given $\delta > 0$, we denote by $\underline{r}(n_\delta)$ the infimum of the radius of the largest inscribed circle of all polygons $B_{\delta, n_\delta, \mathbf{x}}$ for all $\mathbf{x} \in \Omega$, that is

$$(2.16) \quad \underline{r}(n_\delta) = \inf_{\mathbf{x} \in \Omega} r_{\delta, \mathbf{x}},$$

where $r_{\delta, \mathbf{x}}$ (see Figure 3) denotes the radius of the largest inscribed circle (centered on \mathbf{x}) of $B_{\delta, n_\delta, \mathbf{x}}$. We also introduce the notation

$$(2.17) \quad n_\delta = \sup_{\mathbf{x} \in \Omega} n_\delta, \mathbf{x}, \quad \text{and} \quad n_{\delta, \text{inf}} = \inf_{\mathbf{x} \in \Omega} n_\delta, \mathbf{x},$$

and set

$$\gamma_{\delta, n_\delta, \mathbf{x}}(\mathbf{x}, \mathbf{y}) = \begin{cases} \gamma_\delta(\mathbf{x}, \mathbf{y}), & \mathbf{y} \in B_{\delta, n_\delta, \mathbf{x}}, \\ 0, & \mathbf{y} \notin B_{\delta, n_\delta, \mathbf{x}}, \end{cases}$$

which is not symmetric with respect to \mathbf{x} and \mathbf{y} . In order to inherit the symmetry of the original kernel function γ_δ which is crucial to make the nonlocal Green's first identity [13] valid, we define a new series of kernel functions

$$(2.18) \quad \gamma_{\delta, n_\delta}(\mathbf{x}, \mathbf{y}) = \frac{\gamma_{\delta, n_\delta, \mathbf{x}}(\mathbf{x}, \mathbf{y}) + \gamma_{\delta, n_\delta, \mathbf{y}}(\mathbf{y}, \mathbf{x})}{2},$$

which are symmetry with \mathbf{x} and \mathbf{y} , however, not radial. Based on the definition of $\gamma_{\delta, n_\delta}$, we define a new series of nonlocal operators

$$(2.19) \quad \mathcal{L}_{\delta, n_\delta} u(\mathbf{x}) = 2 \int_{\mathbb{R}^2} (u(\mathbf{y}) - u(\mathbf{x})) \gamma_{\delta, n_\delta}(\mathbf{x}, \mathbf{y}) d\mathbf{y} \quad \forall \mathbf{x} \in \Omega.$$

The corresponding series of nonlocal problems is defined as

$$(2.20) \quad \begin{cases} -\mathcal{L}_{\delta, n_\delta} u_{\delta, n_\delta}(\mathbf{x}) = f_\delta(\mathbf{x}) & \text{on } \Omega, \\ u_{\delta, n_\delta}(\mathbf{x}) = 0 & \text{on } \Omega_\delta^c. \end{cases}$$

The nonlocal energy norm associated with $-\mathcal{L}_{\delta, n_\delta}$ is defined as follows

$$\|u(\mathbf{x})\|_{\delta, n_\delta} = \left(\int_{\widehat{\Omega}_\delta} \int_{\widehat{\Omega}_\delta} (u(\mathbf{y}) - u(\mathbf{x}))^2 \gamma_{\delta, n_\delta}(\mathbf{x}, \mathbf{y}) d\mathbf{y} d\mathbf{x} \right)^{1/2}.$$

Obviously,

$$\begin{aligned} \|u(\mathbf{x})\|_{\delta, n_\delta}^2 &= \int_{\widehat{\Omega}_\delta} \int_{\widehat{\Omega}_\delta} (u(\mathbf{y}) - u(\mathbf{x}))^2 \gamma_{\delta, n_\delta, \mathbf{x}}(\mathbf{x}, \mathbf{y}) d\mathbf{y} d\mathbf{x} \\ &= \int_{\widehat{\Omega}_\delta} \int_{\widehat{\Omega}_\delta \cap B_{\delta, n_\delta, \mathbf{x}}} (u(\mathbf{y}) - u(\mathbf{x}))^2 \gamma_\delta(\mathbf{x}, \mathbf{y}) d\mathbf{y} d\mathbf{x}. \end{aligned}$$

3. Discussion on the convergence diagram. To borrow the notion introduced in [42, 43], if u_{δ, n_δ} converges to u_0 for both dashed and dotted arrows in Figure 1, the polygonal approximation is called possessing the AC property. In other words, AC property ensures u_{δ, n_δ} be convergent to u_0 as $\delta \rightarrow 0$ no matter n_δ stays bounded or not.

3.1. Local limit of nonlocal operators with finite and radially symmetric interaction domains. Assume that $\{\delta_k\}_{k=1}^\infty$ is a decreasing sequence and $\delta_k \rightarrow 0$, while u_{δ_k} is the solution of the nonlocal problem (2.2) with $\delta = \delta_k$. From the references [13, 30, 31, 42, 43], we know if $f_{\delta_k} \rightarrow f_0$ in L^2 sense, then $u_{\delta_k} \rightarrow u_0$, while $u_0 \in H_0^1(\Omega)$ satisfies

$$(3.1) \quad \int_{\Omega} \nabla u_0(\mathbf{x}) \nabla \varphi(\mathbf{x}) d\mathbf{x} = \int_{\Omega} f(\mathbf{x}) \varphi(\mathbf{x}) d\mathbf{x}, \quad \forall \varphi \in \mathcal{D}(\Omega),$$

which is the weak form of the local problem (2.5). This result corresponds to the solid arrow in Figure 1 from u_δ to u_0 . We next analyze the convergence property to the local solution u_0 for $u_{\delta_k, n_{\delta_k}}$ which solves the nonlocal problem (2.20) with $\delta = \delta_k$.

3.2. Loss of the AC property with approximate polygonal interaction domains. For $q(\mathbf{x}) = |\mathbf{x}|^2$, simple calculation leads to

$$\mathcal{L}_\delta q(\mathbf{x}) = 2 \int_{B_\delta(\mathbf{0})} |\mathbf{z}|^2 \tilde{\gamma}_\delta(|\mathbf{z}|) d\mathbf{z} = 4, \quad \mathcal{L}_0 q(\mathbf{x}) = 4.$$

On the other hand, by the symmetry of $\gamma_{\delta, n_\delta}$, for all $\mathbf{x} \in \Omega$,

$$\begin{aligned} \mathcal{L}_{\delta, n_\delta} q(\mathbf{x}) &= 2 \int_{B_\delta(\mathbf{x})} (q(\mathbf{y}) - q(\mathbf{x})) \gamma_{\delta, n_\delta}(\mathbf{x}, \mathbf{y}) d\mathbf{y} \\ &= 2 \int_{B_\delta(\mathbf{x})} |\mathbf{y} - \mathbf{x}|^2 \gamma_{\delta, n_\delta}(\mathbf{x}, \mathbf{y}) d\mathbf{y} + 4\mathbf{x} \cdot \int_{B_\delta(\mathbf{x})} (\mathbf{y} - \mathbf{x}) \gamma_{\delta, n_\delta}(\mathbf{x}, \mathbf{y}) d\mathbf{y} \\ &= 2 \int_{B_{\delta, n_\delta, \mathbf{x}}} |\mathbf{y} - \mathbf{x}|^2 \gamma_\delta(\mathbf{x}, \mathbf{y}) d\mathbf{y} = 2 \int_{B_{1, n_\delta, \mathbf{x}}(\mathbf{0})} |\boldsymbol{\xi}|^2 \gamma(\boldsymbol{\xi}) d\boldsymbol{\xi} \\ (3.2) \quad &= 2 \int_{B_{1, n_\delta, \mathbf{x}}(\mathbf{0})} \xi_1^2 \gamma(\boldsymbol{\xi}) d\boldsymbol{\xi} + 2 \int_{B_{1, n_\delta, \mathbf{x}}(\mathbf{0})} \xi_2^2 \gamma(\boldsymbol{\xi}) d\boldsymbol{\xi} \triangleq 2\sigma_{n_\delta, 1}(\mathbf{x}) + 2\sigma_{n_\delta, 2}(\mathbf{x}). \end{aligned}$$

Here the terms $\sigma_{n_\delta, 1}(\mathbf{x})$ and $\sigma_{n_\delta, 2}(\mathbf{x})$ are defined respectively mainly for later use. In this subsection, it is beneficial to consider the summation of them. Now we show that $\mathcal{L}_{\delta, n_\delta} q(\mathbf{x})$ does not converge to $\mathcal{L}_0 q(\mathbf{x})$ when n_δ is uniformly bounded with δ , as $\delta \rightarrow 0$. This means the polygonal approximation does not possess AC property.

THEOREM 3.1. Assume $\{B_{\delta, n_{\delta}, \mathbf{x}}\}$ is a family of polygons which satisfies

$$(3.3) \quad B_{\delta, n_{\delta}, \mathbf{x}} \subset B_{\delta}(\mathbf{x}), \quad \forall \delta, \forall \mathbf{x} \in \Omega.$$

The kernel functions $\gamma_{\delta_k}(\mathbf{x}, \mathbf{y})$ satisfy the conditions (2.3) and (2.4). If n_{δ} is uniformly bounded as $\delta \rightarrow 0$, then $\mathcal{L}_{\delta, n_{\delta}} q(\mathbf{x})$ does not converge to $\mathcal{L}_0 q(\mathbf{x})$ for all $\mathbf{x} \in \Omega$.

Proof. Since n_{δ} is uniformly bounded as $\delta \rightarrow 0$, there exist an integer N such that $n_{\delta} \leq N$ for all δ . We prove the theorem by three steps.

First step, the conclusion is proved under the condition that $\{B_{\delta, n_{\delta}, \mathbf{x}}\}$ is a family of inscribed polygons of $B_{\delta}(\mathbf{x})$. An inscribed polygon of $B_{\delta}(\mathbf{x})$ means all vertices of the polygon lie on the boundary of $B_{\delta}(\mathbf{x})$. In this case the central angle of the longest side of the polygon $B_{1, n_{\delta}, \mathbf{x}}(\mathbf{0})$, denoted by $\theta_{n_{\delta}, \mathbf{x}}$, must be greater than or equal to $2\pi/n_{\delta}$. We consider the sector corresponding to the longest side, which is illustrated in (a) of Figure 4 by the grey triangle and its abutting red cap. The red cap is denoted by $C_{n_{\delta}, \mathbf{x}}$, then $C_{n_{\delta}, \mathbf{x}} \subset B_1(\mathbf{0}) \setminus B_{1, n_{\delta}, \mathbf{x}}(\mathbf{0})$ and

$$|C_{n_{\delta}, \mathbf{x}}| = \frac{1}{2}(\theta_{n_{\delta}, \mathbf{x}} - \sin(\theta_{n_{\delta}, \mathbf{x}})) \geq \frac{1}{2}\left(\frac{2\pi}{n_{\delta}} - \sin\left(\frac{2\pi}{n_{\delta}}\right)\right) \geq \frac{1}{2}\left(\frac{2\pi}{N} - \sin\left(\frac{2\pi}{N}\right)\right),$$

which leads to

$$(3.4) \quad \mathcal{L}_0 q(\mathbf{x}) - \mathcal{L}_{\delta, n_{\delta}} q(\mathbf{x}) = 2 \int_{B_1(\mathbf{0}) \setminus B_{1, n_{\delta}, \mathbf{x}}(\mathbf{0})} |\xi|^2 \gamma(\xi) d\xi \geq 2 \int_{C_{n_{\delta}, \mathbf{x}}} |\xi|^2 \gamma(\xi) d\xi.$$

Then by the condition (2.7), we prove the conclusion.

Second step, if $\{B_{\delta, n_{\delta}, \mathbf{x}}\}$ is a family of convex polygons of $B_{\delta}(\mathbf{x})$. There must exist a family of inscribed polygons of $B_{\delta}(\mathbf{x})$, which contains $\{B_{\delta, n_{\delta}, \mathbf{x}}\}$ and has the same numbers of sides with it, see (b) of Figure 4.

Third step, if $\{B_{\delta, n_{\delta}, \mathbf{x}}\}$ is a family of non-convex polygons of $B_{\delta}(\mathbf{x})$. There must exist a family of convex polygons of $B_{\delta}(\mathbf{x})$, which contains $\{B_{\delta, n_{\delta}, \mathbf{x}}\}$ and has less numbers of sides with it, see (c) of Figure 4. \square

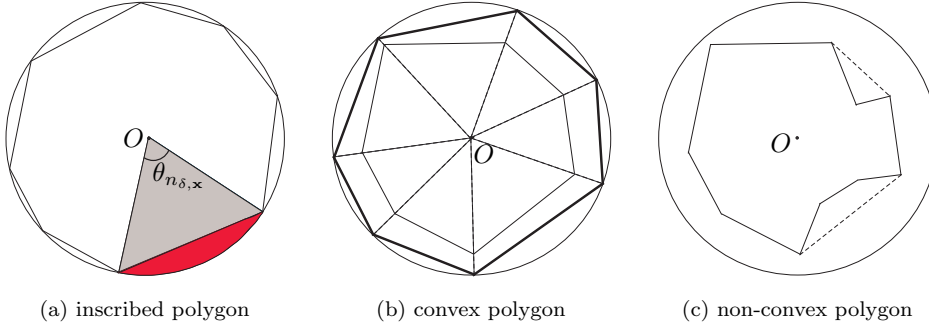


FIG. 4. Different types of polygons in the circle $B_1(\mathbf{0})$

Now we consider a special case where $\mathcal{L}_{\delta, n_{\delta}} q(\mathbf{x})$ converges in pointwise sense, however, to a different limit from $\mathcal{L}_0 q(\mathbf{x})$. In this case, a family of inscribed regular $n_{\delta} \equiv n$ -sided polygons is adopted. Then for any δ and any $\mathbf{x} \in \Omega$, $B_{1, n_{\delta}, \mathbf{x}}(\mathbf{0})$ is a regular n -sided inscribed polygon of $B_1(\mathbf{0})$. Thus

$$(3.5) \quad \mathcal{L}_{\delta, n_{\delta}} q(\mathbf{x}) = 2 \int_{B_{1, n_{\delta}, \mathbf{x}}(\mathbf{0})} |\xi|^2 \gamma(\xi) d\xi < 2 \int_{B_1(\mathbf{0})} |\xi|^2 \gamma(|\xi|) d\xi = 4.$$

This means $\mathcal{L}_{\delta, n_\delta} q(\mathbf{x})$ converges in pointwise sense, however, to a different limit from $\mathcal{L}_0 q(\mathbf{x})$. Such a fact is related to the truncation to the effective nonlocal interaction neighborhood, which has been observed in many computational studies using nonlocal models like the peridynamics. A popular practical strategy to maintain the consistency to the correct limit is through the so-called volume correction algorithms, see for example [33, 51].

In a summary, $\mathcal{L}_{\delta, n_\delta} q(\mathbf{x})$ does not converge to $\mathcal{L}_0 q(\mathbf{x})$ when n_δ is uniformly bounded with δ , as $\delta \rightarrow 0$. In fact, $\mathcal{L}_{\delta, n_\delta} q(\mathbf{x})$ either converges to a wrong limit, or diverges. With either of such cases, it does not blow up.

3.3. Conditional AC property with approximate polygonal interaction domains. One may notice that if $\lim_{\delta \rightarrow 0} n_\delta = \infty$, we may get $\lim_{\delta \rightarrow 0} \sigma_{n_\delta, i}(\mathbf{x}) = 1$, thus

$$(3.6) \quad \lim_{\delta \rightarrow 0} (\mathcal{L}_{\delta, n_\delta} - \mathcal{L}_0) q(\mathbf{x}) = 0, \quad \forall \mathbf{x} \in \Omega.$$

Then u_{δ, n_δ} may converge to u_0 along the dotted arrow in Figure 1 which means the polygonal approximation possesses conditional AC property. We now discuss this convergence issue in the subsequent subsections.

3.3.1. Local-nonlocal Green's formula. As the starting point of the convergence analysis of the local limit, let us first establish an estimate that is referred as a local-nonlocal Green's formula. Indeed, it is derived from the nonlocal Green's formula where part of the integrals are expanded in local forms. As $\delta \rightarrow 0$, it recovers the classical Green's formula.

LEMMA 3.2. (*local-nonlocal Green's formula*). *We have for all $u \in V(\widehat{\Omega}_\delta)$ and $\varphi \in \mathcal{D}(\Omega)$,*

$$(3.7) \quad \int_{\Omega} \varphi(\mathbf{x}) \mathcal{L}_{\delta, n_\delta} u(\mathbf{x}) d\mathbf{x} = \int_{\Omega} u(\mathbf{x}) \sum_{i=1}^2 \sigma_{n_\delta, i}(\mathbf{x}) \partial_{ii}^2 \varphi(\mathbf{x}) d\mathbf{x} + \mathcal{O}(\delta^2) |\varphi|_{4, \infty} \|u\|_{L^1(\Omega)}.$$

Proof. Due to the symmetry of the kernel function $\gamma_{\delta, n_\delta}(\mathbf{x}, \mathbf{y})$ with respect to \mathbf{x} and \mathbf{y} , we have $\forall u \in V(\widehat{\Omega}_\delta)$, and $\varphi \in \mathcal{D}(\Omega)$,

$$\begin{aligned} \int_{\Omega} \varphi(\mathbf{x}) \mathcal{L}_{\delta, n_\delta} u(\mathbf{x}) d\mathbf{x} &= 2 \int_{\Omega} \varphi(\mathbf{x}) \int_{\widehat{\Omega}_\delta} (u(\mathbf{y}) - u(\mathbf{x})) \gamma_{\delta, n_\delta}(\mathbf{x}, \mathbf{y}) d\mathbf{y} d\mathbf{x} \\ &= 2 \int_{\widehat{\Omega}_\delta} \varphi(\mathbf{x}) \int_{\widehat{\Omega}_\delta} (u(\mathbf{y}) - u(\mathbf{x})) \gamma_{\delta, n_\delta}(\mathbf{x}, \mathbf{y}) d\mathbf{y} d\mathbf{x} \\ &= 2 \int_{\widehat{\Omega}_\delta} u(\mathbf{x}) \int_{\widehat{\Omega}_\delta} (\varphi(\mathbf{y}) - \varphi(\mathbf{x})) \gamma_{\delta, n_\delta}(\mathbf{x}, \mathbf{y}) d\mathbf{y} d\mathbf{x} = \int_{\Omega} u(\mathbf{x}) \mathcal{L}_{\delta, n_\delta} \varphi(\mathbf{x}) d\mathbf{x}, \end{aligned}$$

which is in fact a kind of the nonlocal Green's first identity [13], however, for the newly defined nonlocal operator $\mathcal{L}_{\delta, n_\delta}$ other than the original nonlocal operator \mathcal{L}_δ . Since $\varphi \in \mathcal{D}(\Omega)$ is smooth, we can expand the difference $\varphi(\mathbf{y}) - \varphi(\mathbf{x})$ by the Taylor polynomial and then proceed as follows

$$\mathcal{L}_{\delta, n_\delta} \varphi(\mathbf{x}) = 2 \int_{\widehat{\Omega}_\delta} \left(\sum_{|\boldsymbol{\alpha}| \in \mathbb{N}^+} \frac{(\mathbf{y} - \mathbf{x})^\alpha}{\boldsymbol{\alpha}!} d^\alpha \varphi(\mathbf{x}) \right) \gamma_{\delta, n_\delta}(\mathbf{x}, \mathbf{y}) d\mathbf{y}.$$

Since all polynomials $(\mathbf{y} - \mathbf{x})^\alpha$ for odd $|\boldsymbol{\alpha}|$ are odd functions, their products with the

kernel function $\gamma_{\delta, n_\delta}(\mathbf{x}, \mathbf{y})$ vanish identically under the integral. Thus

$$\begin{aligned}\mathcal{L}_{\delta, n_\delta} \varphi(\mathbf{x}) &= 2 \int_{\widehat{\Omega}_\delta} \left(\sum_{|\alpha|=2} \frac{(\mathbf{y}-\mathbf{x})^\alpha}{\alpha!} d^\alpha \varphi(\mathbf{x}) + \sum_{|\alpha|=4} \frac{(\mathbf{y}-\mathbf{x})^\alpha}{\alpha!} d^\alpha \varphi(\boldsymbol{\xi}) \right) \gamma_{\delta, n_\delta}(\mathbf{x}, \mathbf{y}) d\mathbf{y} \\ &= \sum_{i=1}^2 \partial_{i_i}^2 \varphi(\mathbf{x}) \int_{\widehat{\Omega}_\delta} (y_i - x_i)^2 \gamma_{\delta, n_\delta}(\mathbf{x}, \mathbf{y}) d\mathbf{y} + 2 \sum_{|\alpha|=4} \int_{\widehat{\Omega}_\delta} d^\alpha \varphi(\boldsymbol{\xi}) \gamma_{\delta, n_\delta}(\mathbf{x}, \mathbf{y}) \frac{(\mathbf{y}-\mathbf{x})^\alpha}{\alpha!} d\mathbf{y},\end{aligned}$$

where $\boldsymbol{\xi}$ depends on \mathbf{y} and $|\boldsymbol{\xi} - \mathbf{x}| \leq |\mathbf{y} - \mathbf{x}|$. Next, the second term is shown to be of high order. Only the following two kinds of sub-term need to be dealt with, that is

$$\int_{\widehat{\Omega}_\delta} \frac{\partial^4 \varphi(\boldsymbol{\xi})}{\partial x_1^4} (y_1 - x_1)^4 \gamma_{\delta, n_\delta}(\mathbf{x}, \mathbf{y}) d\mathbf{y}, \text{ and } \int_{\widehat{\Omega}_\delta} \frac{\partial^4 \varphi(\boldsymbol{\xi})}{\partial x_1^2 \partial x_2^2} (y_1 - x_1)^2 (y_2 - x_2)^2 \gamma_{\delta, n_\delta}(\mathbf{x}, \mathbf{y}) d\mathbf{y}.$$

For the first kind of sub-term, we have by the condition (2.4)

$$\begin{aligned}\int_{\widehat{\Omega}_\delta} \frac{\partial^4 \varphi(\boldsymbol{\xi})}{\partial x_1^4} (y_1 - x_1)^4 \gamma_{\delta, n_\delta}(\mathbf{x}, \mathbf{y}) d\mathbf{y} &\leq \delta^2 |\varphi|_{4, \infty} \int_{\widehat{\Omega}_\delta} (y_1 - x_1)^2 \gamma_{\delta, n_\delta}(\mathbf{x}, \mathbf{y}) d\mathbf{y} \\ &\leq \delta^2 |\varphi|_{4, \infty} \int_{\widehat{\Omega}_\delta} (y_1 - x_1)^2 \gamma_\delta(\mathbf{x}, \mathbf{y}) d\mathbf{y} = \delta^2 |\varphi|_{4, \infty}.\end{aligned}$$

The second kind of sub-term could be dealt with similarly. Thus,

$$\mathcal{L}_{\delta, n_\delta} \varphi(\mathbf{x}) = \sum_{i=1}^2 \partial_{i_i}^2 \varphi(\mathbf{x}) \int_{\widehat{\Omega}_\delta} (y_i - x_i)^2 \gamma_{\delta, n_\delta}(\mathbf{x}, \mathbf{y}) d\mathbf{y} + \mathcal{O}(\delta^2) |\varphi|_{4, \infty},$$

we then complete the proof by the definition of $\sigma_{n_\delta, i}(\mathbf{x})$ in (3.2). \square

By the definition of $\underline{r}(n_\delta)$ in (2.16), we have for all $u \in V(\widehat{\Omega}_\delta)$,

$$\begin{aligned}(3.8) \quad &\int_{\widehat{\Omega}_\delta} \int_{\widehat{\Omega}_\delta} |u(\mathbf{y}) - u(\mathbf{x})|^2 \gamma_\delta(\mathbf{x}, \mathbf{y}) \chi_{\underline{r}(n_\delta)}(|\mathbf{y} - \mathbf{x}|) d\mathbf{y} d\mathbf{x} \\ &\leq \int_{\widehat{\Omega}_\delta} \int_{\widehat{\Omega}_\delta} |u(\mathbf{y}) - u(\mathbf{x})|^2 \gamma_{\delta, n_\delta}(\mathbf{x}, \mathbf{y}) d\mathbf{y} d\mathbf{x} \\ &\leq \int_{\widehat{\Omega}_\delta} \int_{\widehat{\Omega}_\delta} |u(\mathbf{y}) - u(\mathbf{x})|^2 \gamma_\delta(\mathbf{x}, \mathbf{y}) d\mathbf{y} d\mathbf{x} = \|u(\mathbf{x})\|_\delta^2.\end{aligned}$$

We regard $\gamma_\delta(\mathbf{x}, \mathbf{y}) \chi_{\underline{r}(n_\delta)}(|\mathbf{y} - \mathbf{x}|)$ as a new kernel function, which, like $\gamma_\delta(\mathbf{x}, \mathbf{y})$, induces a norm

$$\|u(\mathbf{x})\|_{\underline{r}(n_\delta)} = \left(\int_{\widehat{\Omega}_\delta} \int_{\widehat{\Omega}_\delta} |u(\mathbf{y}) - u(\mathbf{x})|^2 \gamma_\delta(\mathbf{x}, \mathbf{y}) \chi_{\underline{r}(n_\delta)}(|\mathbf{y} - \mathbf{x}|) d\mathbf{y} d\mathbf{x} \right)^{1/2}.$$

Then from (3.8) we know for all $u \in V(\widehat{\Omega}_\delta)$

$$(3.9) \quad \|u(\mathbf{x})\|_{\underline{r}(n_\delta)} \leq \|u(\mathbf{x})\|_{\delta, n_\delta} \leq \|u(\mathbf{x})\|_\delta,$$

which in fact holds, for all $u \in L^2(\widehat{\Omega}_\delta)$ with $u(\mathbf{x}) = 0$ for $\mathbf{x} \in \Omega_\delta^c$, if terms in (3.9) are allowed to be infinite. Like [2, 3], we prove the corresponding pointwise convergence for $\|u\|_{\delta, n_\delta}^2$ in general d dimensional case under the condition $u \in H^1(\widehat{\Omega}_\delta)$ which is a homogeneous extension from a function in $H_0^1(\Omega)$, see Appendix.

3.3.2. Sufficient conditions to ensure correct local limit. Now, we are ready to show the L^2 -convergence of u_{δ, n_δ} to u_0 as $\delta \rightarrow 0$. For this purpose we need to provide a compactness result and a uniform nonlocal Poincaré-type inequality which enable us to carry on the same convergence proof as in [42, Theorem 2.5]. For brevity we use D to stand for $\widehat{\Omega}_{\delta_0}$ with $\delta_0 \geq \delta$ for all δ or $\delta_0 \geq \delta_k$ for all k , which depends on the situation. This notation is also used in Appendix.

Set $\rho_k(\mathbf{x}, \mathbf{y}) = |\mathbf{y} - \mathbf{x}|^2 \gamma_{\delta_k}(\mathbf{x}, \mathbf{y})$. Since γ_{δ_k} satisfy (2.3) and (2.4), then $\{\rho_k\}$ is a sequence of radial functions and the following property holds for all $\mathbf{x} \in \Omega$

$$(3.10) \quad \begin{cases} \rho_k(\mathbf{x}, \mathbf{y}) \geq 0 \text{ in } \mathbb{R}^2, \\ \int_{\mathbb{R}^2} \rho_k(\mathbf{x}, \mathbf{y}) d\mathbf{y} = 2, \forall k \geq 1, \\ \lim_{k \rightarrow \infty} \int_{|\mathbf{y} - \mathbf{x}| > \varepsilon} \rho_k(\mathbf{x}, \mathbf{y}) d\mathbf{y} = 0, \forall \varepsilon > 0. \end{cases}$$

Thus the following compactness lemma for the norm $\|\cdot\|_\delta$ could be proved, see, e.g. [2, Theorem 4], [34, Theorems 1.2, 1.3] and [29, theorem 5.1].

LEMMA 3.3. [2, 29, 34] Assume $\{u_k\} \subset L^1(D)$ is a bounded sequence such that

$$\int_D \int_D |u_k(\mathbf{y}) - u_k(\mathbf{x})|^2 \gamma_{\delta_k}(\mathbf{x}, \mathbf{y}) d\mathbf{y} d\mathbf{x} \leq C,$$

then $\{u_k\}$ is precompact in $L^2(D)$. Assume that $u_{k_j} \rightarrow u$ in $L^2(D)$, then $u \in H^1(D)$.

In addition we need the following compactness lemma which is similar to Lemma 3.3, however, the kernel function γ_{δ_k} is replaced by $\gamma_{\delta_k, n_{\delta_k}}$.

LEMMA 3.4. Assume $\{u_k\} \subset L^1(D)$ is a bounded sequence and

$$(3.11) \quad \lim_{k \rightarrow \infty} \int_{|\mathbf{y} - \mathbf{x}| \leq r(n_{\delta_k})} (y_i - x_i)^2 \gamma_{\delta_k}(\mathbf{x}, \mathbf{y}) d\mathbf{y} = 1, \quad i = 1, 2.$$

If

$$(3.12) \quad \int_D \int_D |u_k(\mathbf{y}) - u_k(\mathbf{x})|^2 \gamma_{\delta_k, n_{\delta_k}}(\mathbf{x}, \mathbf{y}) d\mathbf{y} d\mathbf{x} \leq C,$$

then $\{u_k\}$ is precompact in $L^2(D)$. Assume that $u_{k_j} \rightarrow u$ in $L^2(D)$, then $u \in H^1(D)$.

Proof. Let $\rho_k(\mathbf{x}, \mathbf{y}) = |\mathbf{y} - \mathbf{x}|^2 \gamma_{\delta_k}(\mathbf{x}, \mathbf{y}) \chi_{\mathcal{I}(n_{\delta_k})}(|\mathbf{y} - \mathbf{x}|)$, by the condition (3.11), (2.3) and (2.4), we know $\{\rho_k\}$ is a sequence of radial functions and for all $\mathbf{x} \in \Omega$,

$$(3.13) \quad \begin{cases} \rho_k(\mathbf{x}, \mathbf{y}) \geq 0 \text{ in } \mathbb{R}^2, \\ \lim_{k \rightarrow \infty} \int_{\mathbb{R}^2} \rho_k(\mathbf{x}, \mathbf{y}) d\mathbf{y} = 2, \\ \lim_{k \rightarrow \infty} \int_{|\mathbf{y} - \mathbf{x}| > \varepsilon} \rho_k(\mathbf{x}, \mathbf{y}) d\mathbf{y} = 0, \forall \varepsilon > 0. \end{cases}$$

The difference between (3.13) and (3.10) is: the second condition of (3.13) takes limit. So we could use similar argument with that in [2, 29, 34] to prove the compactness result if (3.12) is replaced by

$$\|u_k(\mathbf{x})\|_{\mathcal{I}(n_{\delta_k})}^2 = \int_D \int_D |u_k(\mathbf{y}) - u_k(\mathbf{x})|^2 \gamma_{\delta_k}(\mathbf{x}, \mathbf{y}) \chi_{\mathcal{I}(n_{\delta_k})}(|\mathbf{y} - \mathbf{x}|) d\mathbf{y} d\mathbf{x} \leq C.$$

For example, from the proof of [34, Theorems 1.2] we know the essential requirement for $\rho_k(\mathbf{x}, \mathbf{y})$ is: for any $\mathbf{x} \in \Omega$ and fixed $\varepsilon > 0$, there is a k_0 such that

$$\int_{|\mathbf{y}-\mathbf{x}|<\varepsilon} \rho_k(\mathbf{x}, \mathbf{y}) d\mathbf{y} \geq 1/2, \quad \forall k \geq k_0,$$

which is assured by the condition (3.13). Thus we establish the compactness result for the norm $\|\cdot\|_{\underline{r}(n_{\delta_k})}$. Then by the relation (3.9) we complete the proof. \square

LEMMA 3.5. (*Uniform Poincaré-type inequality*). Assume

$$\lim_{k \rightarrow \infty} \int_{|\mathbf{y}-\mathbf{x}| \leq \underline{r}(n_{\delta})} |y_i - x_i|^2 \gamma_{\delta}(\mathbf{x}, \mathbf{y}) d\mathbf{y} = 1, \quad i = 1, 2.$$

Then there exist $\delta_0 > 0$ and $C > 0$ independent of δ such that $\forall \delta < \delta_0$,

$$(3.14) \quad \|u(\mathbf{x})\|_{0,\Omega} \leq C \|u(\mathbf{x})\|_{\underline{r}(n_{\delta})},$$

and thus by (3.9)

$$(3.15) \quad \|u(\mathbf{x})\|_{0,\Omega} \leq C \|u(\mathbf{x})\|_{\delta, n_{\delta}}.$$

The inequality (3.14) is similar to [42, Lemma 3.2], which is a special case of [30, Proposition 5.3] for scalar valued functions. To prove Lemma 3.5, we just need to prove (3.14). From [30] we know the key point is the compactness result, i.e. Lemma 3.4 which has been proved.

THEOREM 3.6. Assume $\{B_{\delta_k, n_{\delta_k}, \mathbf{x}}\}$ is a family of polygons that satisfies (3.3) and

$$(3.16) \quad \lim_{k \rightarrow \infty} \frac{r(n_{\delta_k})}{\delta_k} = 1.$$

If $f_{\delta_k} \rightarrow f_0$ in L^2 sense, the kernel functions $\gamma_{\delta_k}(\mathbf{x}, \mathbf{y})$ satisfy the conditions (2.3) and (2.4), then we have

$$\lim_{k \rightarrow \infty} \|u_{\delta_k, n_{\delta_k}} - u_0\|_{0,\Omega} = 0,$$

where $u_0 \in H_0^1(\Omega)$ is the solution of local problem (3.1).

Proof. By (3.16), (2.3) and (2.4), we know that

$$(3.17) \quad \lim_{k \rightarrow \infty} \int_{|\mathbf{z}| < \underline{r}(n_{\delta_k})} z_i^2 \tilde{\gamma}_{\delta_k}(|\mathbf{z}|) d\mathbf{z} = \lim_{k \rightarrow \infty} \int_{|\mathbf{z}| < \delta_k} z_i^2 \tilde{\gamma}_{\delta_k}(|\mathbf{z}|) d\mathbf{z} = 1, \quad i = 1, 2.$$

That is the condition (3.11) holds.

Take $\delta = \delta_k$ in (2.20) and multiply $u_{\delta_k, n_{\delta_k}}$ in both sides, we get

$$\|u_{\delta_k, n_{\delta_k}}\|_{\delta_k, n_{\delta_k}}^2 = - \int_{\Omega} u_{\delta_k, n_{\delta_k}} \mathcal{L}_{\delta_k, n_{\delta_k}} u_{\delta_k, n_{\delta_k}} d\mathbf{x} = \int_{\Omega} f_{\delta_k} u_{\delta_k, n_{\delta_k}} d\mathbf{x}.$$

Then by the Cauchy-Schwarz inequality and nonlocal Poincaré-type inequality (3.15) in Lemma 3.5,

$$\|u_{\delta_k, n_{\delta_k}}\|_{\delta_k, n_{\delta_k}}^2 \leq \|f_{\delta_k}\|_{0,\Omega} \|u_{\delta_k, n_{\delta_k}}\|_{0,\Omega} \leq C \|f_{\delta_k}\|_{0,\Omega} \|u_{\delta_k, n_{\delta_k}}\|_{\delta_k, n_{\delta_k}}.$$

Thus $\|u_{\delta_k, n_{\delta_k}}\|_{\delta_k, n_{\delta_k}} \leq C \|f_{\delta_k}\|_{0, \Omega}$ holds. This, together with $f_{\delta_k} \rightarrow f_0$, leads to the following uniform boundedness result

$$(3.18) \quad \|u_{\delta_k, n_{\delta_k}}\|_{\delta_k, n_{\delta_k}} \leq C' \|f_0\|_{0, \Omega},$$

where $C' > 0$ is a constant independent of δ_k . Then by [Lemma 3.4](#), we get the convergence of a subsequence of $\{u_{\delta_k, n_{\delta_k}}\}$ in L^2 to a limit point $u_0 \in H_0^1(\Omega)$. For the brevity, we use the same symbol to denote the subsequence.

On the other hand, from [\(3.7\)](#), we know for all $\varphi \in \mathcal{D}(\Omega)$,

$$\begin{aligned} \int_{\Omega} \varphi(\mathbf{x}) \mathcal{L}_{\delta_k, n_{\delta_k}} u_{\delta_k, n_{\delta_k}}(\mathbf{x}) d\mathbf{x} &= \int_{\Omega} u_{\delta_k, n_{\delta_k}}(\mathbf{x}) \left(\sum_{i=1}^2 \sigma_{n_{\delta_k}, i}(\mathbf{x}) \partial_{ii}^2 \varphi(\mathbf{x}) \right) d\mathbf{x} \\ &\quad + \mathcal{O}(\delta_k^2) |\varphi|_{4, \infty} \|u_{\delta_k, n_{\delta_k}}\|_{L^1(\Omega)}. \end{aligned}$$

Thus by the uniform boundedness result [\(3.18\)](#) and the uniform Poincaré-type inequality [\(3.15\)](#) in [Lemma 3.5](#), the following formula holds for all $\varphi \in \mathcal{D}(\Omega)$,

$$(3.19) \quad \int_{\Omega} u_{\delta_k, n_{\delta_k}}(\mathbf{x}) \left(\sum_{i=1}^2 \sigma_{n_{\delta_k}, i}(\mathbf{x}) \partial_{ii}^2 \varphi(\mathbf{x}) \right) d\mathbf{x} + \mathcal{O}(\delta_k^2) = - \int_{\Omega} f_{\delta_k}(\mathbf{x}) \varphi(\mathbf{x}) d\mathbf{x}.$$

From the condition [\(3.3\)](#) and the definition of $r(n_{\delta_k})$, we know for all $\mathbf{x} \in \Omega$

$$\int_{|\mathbf{z}| < r(n_{\delta_k})} z_i^2 \tilde{\gamma}_{\delta_k}(|\mathbf{z}|) d\mathbf{z} \leq \sigma_{n_{\delta_k}, i}(\mathbf{x}) \leq \int_{|\mathbf{z}| < \delta_k} z_i^2 \tilde{\gamma}_{\delta_k}(|\mathbf{z}|) d\mathbf{z}, \quad i = 1, 2,$$

then by [\(3.17\)](#) and the squeeze theorem, the following limit result holds

$$(3.20) \quad \lim_{k \rightarrow \infty} \sigma_{n_{\delta_k}, i}(\mathbf{x}) = 1, \quad i = 1, 2, \quad \forall \mathbf{x} \in \Omega.$$

Taking limit in [\(3.19\)](#), we know u_0 satisfies [\(3.1\)](#), thus the proof is completed. \square

The condition for [Theorem 3.6](#) is general. In this paper, we also establish two other theorems which need stronger conditions, however, apply to many circumstances.

THEOREM 3.7. *Assume $\{B_{\delta_k, n_{\delta_k}, \mathbf{x}}\}$ is a family of convex polygons which satisfies [\(3.3\)](#) and*

$$(3.21) \quad \inf_{\mathbf{x} \in \Omega} \frac{|B_{\delta_k, n_{\delta_k}, \mathbf{x}}|}{|B_{\delta_k}(\mathbf{x})|} \rightarrow 1 \quad \text{as } k \rightarrow \infty.$$

If $f_{\delta_k} \rightarrow f_0$ in L^2 sense, $\gamma_{\delta_k}(\mathbf{x}, \mathbf{y})$ satisfy the conditions [\(2.3\)](#) and [\(2.4\)](#), the same conclusion as [Theorem 3.6](#) holds.

Proof. According to [Theorem 3.6](#), we need to prove [\(3.16\)](#) by [\(3.21\)](#) and the condition ‘convex’. We prove this by contradiction. If [\(3.16\)](#) does not hold, then there exists a constant $\varepsilon_0 \in (0, 1/2)$ such that for all k , $r(n_{\delta_k})/\delta_k \leq 1 - 2\varepsilon_0$. From the definition of $r(n_{\delta_k})$, for any k there exists a point $\mathbf{x}_0 \in \Omega$ such that $r_{\delta_k, \mathbf{x}_0}/\delta_k \leq 1 - \varepsilon_0$. Assume the inscribed circle is tangent to the polygon at point P which is on the side $\overline{A_1 A_2}$. The side $\overline{A_1 A_2}$ must be a part of a chord, which is denoted by $\overline{A_3 A_4}$, see (a) of [Figure 5](#). Denote the cap corresponding to the chord $\overline{A_3 A_4}$ by C_{grey} which is the cap with grey color in (a) of [Figure 5](#). Since the polygon $B_{\delta_k, n_{\delta_k}, \mathbf{x}_0}$ is convex, $C_{\text{grey}} \subset$

$B_{\delta_k}(\mathbf{x}_0) \setminus B_{\delta_k, n_{\delta_k}, \mathbf{x}_0}$. The circle, polygon and cap are mapped to their counterparts in $B_1(\mathbf{0})$ by the mapping (2.15), see (b) of Figure 5 where the image of C_{grey} is denoted by $\widehat{C}_{\text{grey}}$. Thus,

$$(3.22) \quad \widehat{C}_{\text{grey}} \subset B_1(\mathbf{0}) \setminus B_{1, n_{\delta_k}, \mathbf{x}_0}(\mathbf{0}).$$

By simple calculation, we have

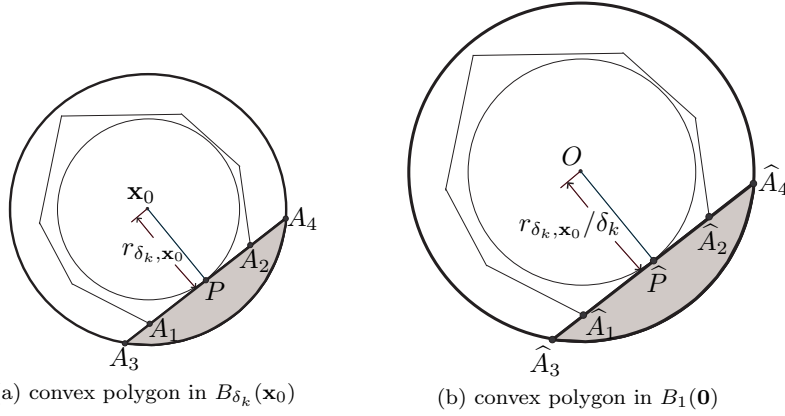


FIG. 5. Convex polygon in the circle $B_{\delta_k}(\mathbf{x}_0)$ and its image by the mapping (2.15)

$$|\widehat{C}_{\text{grey}}| = \theta_{n_{\delta_k}, \mathbf{x}_0} - \sin(\theta_{n_{\delta_k}, \mathbf{x}_0}),$$

with

$$\theta_{n_{\delta_k}, \mathbf{x}_0} = 2 \arccos(r_{\delta_k, \mathbf{x}_0}/\delta_k) \geq 2 \arccos(1 - \varepsilon_0),$$

which leads to

$$(3.23) \quad |\widehat{C}_{\text{grey}}| \geq 2 \arccos(1 - \varepsilon_0) - \sin(2 \arccos(1 - \varepsilon_0)).$$

Thus by (3.22) and (3.23) we know for any k there exists a point $\mathbf{x}_0 \in \Omega$ such that

$$\frac{|B_{\delta_k, n_{\delta_k}, \mathbf{x}_0}|}{|B_{\delta_k}(\mathbf{x}_0)|} = \frac{|B_{1, n_{\delta_k}, \mathbf{x}_0}|}{|B_1(\mathbf{0})|} \leq 1 - \widehat{C}_{\text{grey}} \leq 1 - 2 \arccos(1 - \varepsilon_0) + \sin(2 \arccos(1 - \varepsilon_0)),$$

which contradicts the condition (3.21). \square

3.3.3. Local limit as $n_{\delta} \rightarrow \infty$ for quasi-uniform inscribed polygons. If the family of polygons possesses ‘inscribed’ and ‘quasi-uniform’ properties, the condition (3.21) could be further simplified.

DEFINITION 3.8. A family of polygons $\{B_{\delta, n_{\delta}, \mathbf{x}}\}$ is called quasi-uniform if there exist two constants C_1 and $C_2 > 0$ such that $\forall \delta > 0$, the following two bounds hold

$$\sup_{\mathbf{x} \in \Omega} \frac{H_{n_{\delta}, \mathbf{x}}^{\max}}{H_{n_{\delta}, \mathbf{x}}^{\min}} \leq C_1, \quad \forall \mathbf{x} \in \Omega,$$

where $H_{n_{\delta}, \mathbf{x}}^{\max}$ and $H_{n_{\delta}, \mathbf{x}}^{\min}$ stand for the lengths of the longest and shortest sides of the polygon $B_{\delta, n_{\delta}, \mathbf{x}}$, respectively, and

$$\sup_{\mathbf{x} \in \Omega} \frac{\delta}{r_{\delta, \mathbf{x}}} \leq C_2, \quad \forall \mathbf{x} \in \Omega.$$

Then for a quasi-uniform family of polygons, there exists a constant $C > 0$ such that for all $\delta > 0$, $n_{\delta} \leq Cn_{\delta, \inf}$ holds.

THEOREM 3.9. *Assume $\{B_{\delta_k, n_{\delta_k}, \mathbf{x}}\}$ is a quasi-uniform family of inscribed polygons. The kernel functions satisfy (2.3) and (2.4). If $f_{\delta_k} \rightarrow f_0$ in L^2 sense, and*

$$(3.24) \quad \lim_{k \rightarrow \infty} n_{\delta_k} = \infty,$$

then we have $\lim_{k \rightarrow \infty} \|u_{\delta_k, n_{\delta_k}} - u_0\|_{0, \Omega} = 0$.

Proof. By (3.24) and the quasi-uniformity of $\{B_{\delta_k, n_{\delta_k}, \mathbf{x}}\}$, we know that

$$(3.25) \quad n_{\delta_k, \mathbf{x}} \geq n_{\delta_k, \inf} \geq \frac{1}{C} n_{\delta_k} \rightarrow \infty, \quad \forall \mathbf{x} \in \Omega,$$

and thus (3.21) holds. Then by Theorem 3.7 we complete the proof. \square

REMARK 3.10. *As a typical example, for a family of regular inscribed polygons, if (3.24) holds, we have $r(n_{\delta_k}) = \delta_k \cos \frac{\pi}{n_{\delta_k}}$. Thus (3.16) holds obviously.*

3.4. Examples of kernel function. Some popular types of kernel function satisfy the conditions (2.3), (2.4). Here we list two special types of them for general d dimensional setting, however, the classification is not strict. For more discussions on the effects of the kernels on the nonlocal models, we refer to [11, 35].

Type 1. Integrable kernel, for example,

Type 1.1 Constant kernel:

$$(3.26) \quad \gamma(t) = \frac{d(d+2)}{w_d}, \quad \text{for } 0 < t \leq 1,$$

where w_d is the surface area of the unit sphere in \mathbb{R}^d .

Type 1.2 Linear kernel:

$$\gamma(t) = \frac{d(d+2)(d+3)}{w_d}(1-t), \quad \text{for } 0 < t \leq 1.$$

Type 1.3 Exponential kernel (Gaussian-like):

$$\gamma(t) = \frac{d}{C_e w_d} e^{-t^2}, \quad \text{for } 0 < t \leq 1, \quad \text{with } C_e = \int_0^1 \tau^3 e^{-\tau^2} d\tau = 2^{-1} - e^{-1}.$$

Type 2. Singular (at the origin) kernel:

$$\gamma(t) = \frac{d(d+2-s)}{w_d} t^{-s} \quad \text{for } 0 < t \leq 1,$$

which stands for different kernel for different s . For $s \in (d, d+2)$ it is fractional kernel, for $s = 1$ it is Peridynamics kernel [37], for $s \in (d-1, d)$ it is in fact integrable.

3.5. Higher dimensional cases. So far most of the discussions are carried out for two dimensional case. Now we extend the established results to general high dimensional case. In fact, [Theorem 3.6](#) and [Theorem 3.7](#) are stated and indeed valid in any high dimensional case subject to the corresponding conditions on the kernels and with the polygonal approximations of the circle changed to polyhedral approximations of the sphere. Meanwhile, modifications and extensions of [Theorem 3.9](#) and [Remark 3.10](#) in high dimensional settings need to be further investigated.

4. Numerical results and discussions. While most of the earlier discussions are analytical nature and focused on operators and problems defined on the continuum level. We provide some numerical results here to provide further illustrations.

EXAMPLE 4.1. We consider the nonlocal problem (2.2) and the truncated nonlocal problem (2.20) on the domain $\Omega = (0, 1)^2$ with the constant kernel function (2.12) which is the two dimensional case of (3.26). The truncated nonlocal operator $\mathcal{L}_{\delta, n_\delta}$ in (2.20) is defined by the strategy $\sharp = \text{nocaps}$ to approximate balls. Note that, for

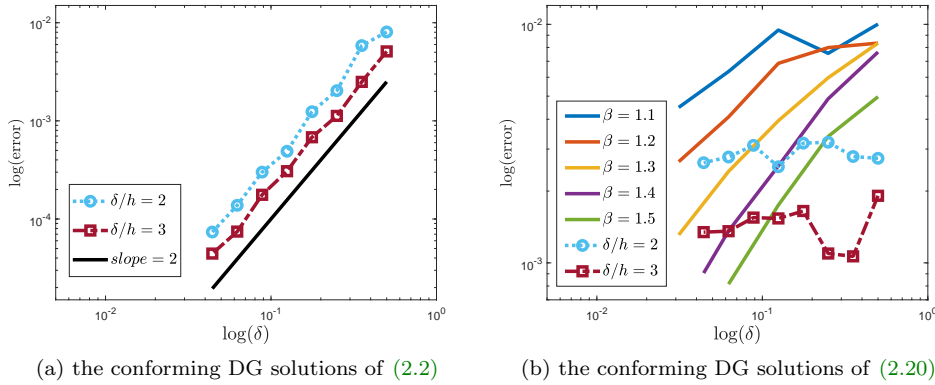


FIG. 6. L^2 error between the conforming DG solutions and the exact local solution

$\mathbf{x} \in \Omega$, $\mathcal{L}_\delta u_\delta(\mathbf{x}) = \Delta u_\delta(\mathbf{x})$ for $\delta \geq 0$ and polynomials $u_\delta(\mathbf{x})$, $\mathbf{x} \in \widehat{\Omega}_\delta$ with order up to three [10, 45]. As in [10] the manufactured solution $u_\delta(\mathbf{x}) = x_1^2 x_2 + x_2^2$ is used to obtain the right hand side function $f_\delta(\mathbf{x}) = -\Delta u_\delta = -2(x_2 + 1)$ for $\mathbf{x} \in \Omega$.

In fact the solution of corresponding local problem (3.1) is $u_0(\mathbf{x}) = u_\delta(\mathbf{x})|_\Omega = x_1^2 x_2 + x_2^2$. The nonlocal problem (2.2) and (2.20) are all approximated by the conforming DG method proposed in [16] which does not require the solution be continuous across $\partial\Omega$, while in [10] the authors use continuous linear finite element method on $\widehat{\Omega}_\delta$ which is described in subsection 2.2. Since the nonlocal solution $u_\delta(\mathbf{x})$ is continuous across $\partial\Omega$ in this example, there is almost no difference between the two types of finite element approximation. However, for those nonlocal solution discontinuous across $\partial\Omega$, the conforming DG method still performs well, while the continuous linear finite element method is no longer efficient.

Since $\mathcal{L}_{\delta, n_\delta}$ is defined by the strategy $\sharp = \text{nocaps}$, we denote the corresponding conforming DG solution of (2.20) as $u_{\delta, n_\delta}^{\text{D, nocaps}}$. To get the conforming DG solution of (2.2), one-point centroid rule is used for approximating the integrals related to those caps, the resultant solution is denoted by $u_\delta^{\text{D, exactcaps}}$ (the word ‘exactcaps’ is used according to [10]).

Then we report on the convergence of the two sequences of conforming DG so-

lutions to the given exact local solution with respect to the L^2 -norm on Ω . From left panel of [Figure 6](#), we see that if the ratio δ/h is fixed, the convergence rate for $u_\delta^{\text{D,exactcaps}}$ is of second order. This is not surprising at all since appropriate numerical quadrature is used to approximate the original conforming DG discretization. While from the right panel of [Figure 6](#), we see that for fixed δ/h , the error of $u_{\delta,n_\delta}^{\text{D,nocaps}}$ hardly shows any drop. On the other hand, if $h = \mathcal{O}(\delta^\beta)$ is used with $\beta > 1$ we do find the positive convergence rates which depend on β .

These experimental findings are consistent to the results of earlier analysis. We now provide some further explanations. The strategy $\sharp = \text{nocaps}$ uses inscribed polygonal $B_{\delta,n_\delta,\mathbf{x}}$ to approximate the exact ball $B_\delta(\mathbf{x})$. For fixed δ/h and quasi-uniform triangulation, we have for all $\delta, n_\delta \leq N$ with $N \sim \mathcal{O}(\delta/h)$, then by [Theorem 3.1](#),

$$(4.1) \quad u_{\delta,n_\delta} \not\rightarrow u_0, \text{ as } \delta \rightarrow 0.$$

Since the conforming DG method is an AC scheme [\[16\]](#), we have

$$(4.2) \quad u_{\delta,n_\delta}^{\text{D,nocaps}} - u_{\delta,n_\delta} \rightarrow 0, \text{ as } \delta \rightarrow 0,$$

which, together with [\(4.1\)](#), implies that $\{u_{\delta,n_\delta}^{\text{D,nocaps}}\}$ does not converge to u_0 as $\delta \rightarrow 0$.

For the case $h = \mathcal{O}(\delta^\beta)$ with $\beta > 1$ and quasi-uniform triangulation, the condition $\delta/h \rightarrow \infty$ holds as $\delta \rightarrow 0$, thus [\(3.24\)](#) holds. Then by [Theorem 3.9](#) we know

$$u_{\delta,n_\delta} \rightarrow u_0, \text{ as } \delta \rightarrow 0,$$

which, together with [\(4.2\)](#), implies that $\{u_{\delta,n_\delta}^{\text{D,nocaps}}\}$ converges to u_0 as $\delta \rightarrow 0$.

Next, we extend the results above to the other cases in [\(2.9\)](#) besides $\sharp = \text{nocaps}$. The strategy $\sharp = \text{regular}$ is a special case of $\sharp = \text{nocaps}$. The strategy $\sharp = \text{approx caps}$ also uses inscribed polygons to approximate the exact ball, the conclusion is similar to that of $\sharp = \text{nocaps}$. To be specific, for bounded δ/h and quasi-uniform triangulation, if the number of sub-triangles that approximate the caps is also bounded, then by [Theorem 3.1](#) the conforming DG solution does not converge to the exact local solution as $\delta \rightarrow 0$. On the other hand, if the number of sub-triangles tends to infinity as $\delta \rightarrow 0$, thus [\(3.24\)](#) holds, then by [Theorem 3.9](#) we know the conforming DG solution converges to the exact local solution as $\delta \rightarrow 0$. For the strategy $\sharp = \text{3vertices}$: if δ/h is uniformly bounded as $\delta \rightarrow 0$, then by [Theorem 3.1](#) the non-convergence is established. If δ/h tends to infinity as $\delta \rightarrow 0$, we can not use [Theorem 3.7](#) or [Theorem 3.9](#) since the polygons are not convex. However, we could use [Theorem 3.6](#) to prove $u_{\delta,n_\delta}^{\text{D,3vertices}}$ converges to u_0 as $\delta \rightarrow 0$. In fact, for quasi-uniform triangulation we have

$$\lim_{\delta \rightarrow 0} \frac{r(n_\delta)}{\delta} \geq \lim_{\delta \rightarrow 0} \frac{\delta - h}{\delta} = 1,$$

which means [\(3.16\)](#) holds.

For the rest types of polygonal approximations of Euclidean balls in [\(2.9\)](#), i.e.

$$(4.3) \quad \sharp \in \{123\text{vertices}, 23\text{vertices}, \text{barycenter}\},$$

the corresponding families of polygons are no longer contained in corresponding Euclidean balls, that is the condition [\(3.3\)](#) does not hold. However, the analysis is similar to that derived in this paper, with consideration for the extension rule of the original kernel function to the outside of the interaction domain.

As we indicated earlier, there is almost no difference between the conforming DG and continuous linear finite element method for this example. The conclusion for $u_{\delta, n_\delta}^{D, \#}$ also holds for $u_{\delta, n_\delta}^{h, \#}$. We summarize it as: for all types of polygonal approximations of Euclidean balls listed in (2.9), if the ratio δ/h is fixed or bounded from above, neither $\|u_\delta^h - u_{\delta, n_\delta}^{h, \#}\|_{L^2}$ nor $\|u_0 - u_{\delta, n_\delta}^{h, \#}\|_{L^2}$ would converge to zero as $\delta \rightarrow 0$.

5. Conclusion. We discussed in this paper some new nonlocal operators which, on the continuum level, are approximations of the nonlocal operators with radially symmetric kernel functions. They are defined through a family of polygons that approximate the interaction domain of the original operator. It is well known that the original nonlocal operators converge to the local operator, at the same time the convergence for the nonlocal solutions to the local one is also well established. However, as shown in subsection 3.2, the new nonlocal operators may not converge to the local operator as δ vanishes if the number of sides of the polygons, n_δ , is uniformly bounded. This phenomenon is interpreted as losing AC property for the polygonal approximation. We proved that the new nonlocal solutions converge to the local solution if n_δ tends to infinite as $\delta \rightarrow 0$, which means the polygonal approximation possesses conditional AC property. In section 4 the numerical experiments in [10] were reproduced, but with some modifications to test the conditional AC property if the Euclidian balls are approximated by throwing away those caps. Our findings suggest two options to ensure the new nonlocal solutions converge to the right local limit: (i) keep those caps and use appropriate numerical quadrature to calculate the related integrals, (ii) throw away those caps or approximate them by some sub-triangles, however, use $h = o(\delta)$. The suggestion is not only suitable for finite element methods, but also applies to other mesh dependent numerical schemes, such as finite difference and collocation methods.

The current study focuses on the convergence of the nonlocal solutions u_{δ, n_δ} to the local one. However, when some specific numerical schemes are used, one critical question is how the convergence order depends on β with respect to the vanishing parameter. This issue is briefly mentioned in section 4 where we can see from the right panel of Figure 6 that the convergence orders depend on β . In fact one may derive estimates like (2.14) as mentioned earlier, see details in a subsequent work [15]. Naturally, extensions to higher dimensions and to nonlinear and time-dependent problems, as well as studies on the coupling with suitable quadrature schemes, will also be questions that remain to be further studied.

Appendix A. The limiting behavior of the norm.

THEOREM A.1. *Assume the kernel functions γ_{δ_k} satisfy the conditions (2.3) and (2.4). We have the following pointwise limit*

$$(A.1) \quad \lim_{k \rightarrow \infty} \int_D \int_D |u(\mathbf{y}) - u(\mathbf{x})|^2 \gamma_{\delta_k}(\mathbf{x}, \mathbf{y}) d\mathbf{y} d\mathbf{x} = \int_D |\nabla u(\mathbf{x})|^2 d\mathbf{x}.$$

Proof. Let $\rho_k(\mathbf{x}, \mathbf{y}) = |\mathbf{y} - \mathbf{x}|^2 \gamma_{\delta_k}(\mathbf{x}, \mathbf{y})$, then $\{\rho_k\}$ is a sequence of radial functions and satisfies the conditions (3.10). From [2, Corollary 1] or [3, Theorem 2], we know

$$\lim_{k \rightarrow \infty} \int_D \int_D \frac{|u(\mathbf{y}) - u(\mathbf{x})|^2}{|\mathbf{y} - \mathbf{x}|^2} \rho_k(\mathbf{x}, \mathbf{y}) d\mathbf{y} d\mathbf{x} = \int_D |\nabla u(\mathbf{x})|^2 d\mathbf{x},$$

which is in fact (A.1), we then complete the proof. \square

THEOREM A.2. Under the condition of [Theorem A.1](#), and assume the counterpart in d dimensional case of [\(3.11\)](#) holds, we have the following pointwise limit

$$\lim_{k \rightarrow \infty} \int_D \int_D |u(\mathbf{y}) - u(\mathbf{x})|^2 \gamma_{\delta_k}(\mathbf{x}, \mathbf{y}) \chi_{\underline{r}(n_{\delta_k})}(|\mathbf{y} - \mathbf{x}|) d\mathbf{y} d\mathbf{x} = \int_D |\nabla u(\mathbf{x})|^2 d\mathbf{x}.$$

Proof. From the proof of [[2](#), Theorem 2], we just need to give the proof for $u \in C^2(\bar{D})$. In this situation,

$$|u(\mathbf{y}) - u(\mathbf{x})| = |(\mathbf{y} - \mathbf{x}) \cdot \nabla u(\mathbf{x})| + o(|\mathbf{y} - \mathbf{x}|^2).$$

For each fixed $\mathbf{x} \in \Omega$,

$$\int_D |u(\mathbf{y}) - u(\mathbf{x})|^2 \gamma_{\delta_k}(\mathbf{x}, \mathbf{y}) \chi_{\underline{r}(n_{\delta_k})}(|\mathbf{y} - \mathbf{x}|) d\mathbf{y} = \int_{|\mathbf{y} - \mathbf{x}| < \text{dist}(\mathbf{x}, \partial D)} + \int_{|\mathbf{y} - \mathbf{x}| \geq \text{dist}(\mathbf{x}, \partial D)}.$$

The second integral tends to 0 as $k \rightarrow \infty$. Set $R = \text{dist}(\mathbf{x}, \partial D)$, when $\underline{r}(n_{\delta_k}) \leq R$,

$$\begin{aligned} & \int_{|\mathbf{y} - \mathbf{x}| < R} |u(\mathbf{y}) - u(\mathbf{x})|^2 \gamma_{\delta_k}(\mathbf{x}, \mathbf{y}) \chi_{\underline{r}(n_{\delta_k})}(|\mathbf{y} - \mathbf{x}|) d\mathbf{y} \\ &= \int_{|\mathbf{z}| < \underline{r}(n_{\delta_k})} \left(|\mathbf{z} \cdot \nabla u(\mathbf{x})|^2 + o(r^2) \right) \tilde{\gamma}_{\delta_k}(|\mathbf{z}|) d\mathbf{z} \\ &= \int_{|\mathbf{z}| < \underline{r}(n_{\delta_k})} |\mathbf{z} \cdot \nabla u(\mathbf{x})|^2 \tilde{\gamma}_{\delta_k}(|\mathbf{z}|) d\mathbf{z} + \int_0^{\underline{r}(n_{\delta_k})} \rho_k(r) \int_{|\mathbf{z}|=r} o(r^2) d\mathbf{S}_{d-1} dr \\ &= \sum_{i=1}^d (\partial_i u(\mathbf{x}))^2 \int_{|\mathbf{z}| < \underline{r}(n_{\delta_k})} z_i^2 \tilde{\gamma}_{\delta_k}(|\mathbf{z}|) d\mathbf{z} + o\left(\int_0^{\underline{r}(n_{\delta_k})} r^{d+1} \tilde{\gamma}_{\delta_k}(r) dr \right). \end{aligned}$$

From the second condition of [\(2.4\)](#) and [\(3.11\)](#), we know that

$$\lim_{k \rightarrow \infty} \int_{|\mathbf{z}| < \underline{r}(n_{\delta_k})} z_i^2 \tilde{\gamma}_{\delta_k}(|\mathbf{z}|) d\mathbf{z} = \lim_{k \rightarrow \infty} \int_{|\mathbf{z}| < \delta_k} z_i^2 \tilde{\gamma}_{\delta_k}(|\mathbf{z}|) d\mathbf{z} = 1, \quad i = 1, 2, \dots, d.$$

Thus

$$\lim_{k \rightarrow \infty} \int_D |u(\mathbf{y}) - u(\mathbf{x})|^2 \gamma_{\delta_k}(\mathbf{x}, \mathbf{y}) \chi_{\underline{r}(n_{\delta_k})}(|\mathbf{y} - \mathbf{x}|) d\mathbf{y} = |\nabla u(\mathbf{x})|^2. \quad \square$$

THEOREM A.3. Under the condition of [Theorem A.2](#), we have the pointwise limit

$$(A.2) \quad \lim_{k \rightarrow \infty} \int_D \int_D |u(\mathbf{y}) - u(\mathbf{x})|^2 \gamma_{\delta_k, n_{\delta_k}}(\mathbf{x}, \mathbf{y}) d\mathbf{y} d\mathbf{x} = \int_D |\nabla u(\mathbf{x})|^2 d\mathbf{x}.$$

This means $\lim_{k \rightarrow \infty} \|u(\mathbf{x})\|_{\delta_k, n_{\delta_k}}^2 = \int_D |\nabla u(\mathbf{x})|^2 d\mathbf{x}$.

Proof. By [\(3.9\)](#), that is $\forall u \in V(\hat{\Omega}_{\delta_k})$, $\|u(\mathbf{x})\|_{\underline{r}(n_{\delta_k})} \leq \|u(\mathbf{x})\|_{\delta_k, n_{\delta_k}} \leq \|u(\mathbf{x})\|_{\delta_k}$. Together with [Theorem A.1](#), [Theorem A.2](#), and the squeeze theorem we prove [\(A.2\)](#). \square

REFERENCES

- [1] P. W. BATES AND A. CHMAJ, *An integrodifferential model for phase transitions: stationary solutions in higher space dimensions*, Journal of Statistical Physics, 95 (1999), pp. 1119–1139.

- [2] J. BOURGAIN, H. BREZIS, AND P. MIRONESCU, *Another look at sobolev spaces*, in *Optimal Control and Partial Differential Equations*, JL Menaldi, E. Rofman, A. Sulem (Eds.), a volume in honor of A. Bensoussan's 60th birthday, IOS Press, Amsterdam, 2001.
- [3] H. BREZIS, *How to recognize constant functions. connections with sobolev spaces*, *Russian Mathematical Surveys*, 57 (2002), pp. 693–708.
- [4] A. BUADES, B. COLL, AND J.-M. MOREL, *Image denoising methods. a new nonlocal principle*, *SIAM Review*, 52 (2010), pp. 113–147.
- [5] N. BURCH, M. D'ELIA, AND R. B. LEHOUCQ, *The exit-time problem for a markov jump process*, *The European Physical Journal Special Topics*, 223 (2014), pp. 3257–3271.
- [6] C. CORTAZAR, M. ELGUETA, J. D. ROSSI, AND N. WOLANSKI, *How to approximate the heat equation with neumann boundary conditions by nonlocal diffusion problems*, *Archive for Rational Mechanics and Analysis*, 187 (2008), pp. 137–156.
- [7] A. H. DELGOSHAIE, D. W. MEYER, P. JENNY, AND H. A. TCHELEPI, *Non-local formulation for multiscale flow in porous media*, *Journal of Hydrology*, 531 (2015), pp. 649–654.
- [8] M. D'ELIA, Q. DU, C. GLUSA, M. GUNZBURGER, X. TIAN, AND Z. ZHOU, *Numerical methods for nonlocal and fractional models*, *Acta Numerica*, 29 (2020), pp. 1–124.
- [9] M. D'ELIA, Q. DU, M. GUNZBURGER, AND R. LEHOUCQ, *Nonlocal convection-diffusion problems on bounded domains and finite-range jump processes*, *Computational Methods in Applied Mathematics*, 17 (2017), pp. 707–722.
- [10] M. D'ELIA, M. GUNZBURGER, AND C. VOLLMANN, *A cookbook for approximating euclidean balls and for quadrature rules in finite element methods for nonlocal problems*, *Mathematical Models and Methods in Applied Sciences*, (2021), pp. 1–63.
- [11] Q. DU, *Nonlocal modeling, analysis and computation*, SIAM, 2019.
- [12] Q. DU, M. GUNZBURGER, R. B. LEHOUCQ, AND K. ZHOU, *Analysis and approximation of nonlocal diffusion problems with volume constraints*, *SIAM Review*, 54 (2012), pp. 667–696.
- [13] Q. DU, M. GUNZBURGER, R. B. LEHOUCQ, AND K. ZHOU, *A nonlocal vector calculus, non-local volume-constrained problems, and nonlocal balance laws*, *Mathematical Models and Methods in Applied Sciences*, 23 (2013), pp. 493–540.
- [14] Q. DU, Y. TAO, X. TIAN, AND J. YANG, *Asymptotically compatible discretization of multidimensional nonlocal diffusion models and approximation of nonlocal green's functions*, *IMA Journal of numerical analysis*, 39 (2019), pp. 607–625.
- [15] Q. DU, H. XIE, X. YIN, AND J. ZHANG, *Tba*, TBA, Submitted (***)
- [16] Q. DU AND X. YIN, *A conforming dg method for linear nonlocal models with integrable kernels*, *Journal of Scientific Computing*, 80 (2019), pp. 1913–1935.
- [17] Q. DU, J. ZHANG, AND C. ZHENG, *On uniform second order nonlocal approximations to linear two-point boundary value problems*, *Communications in Mathematical Sciences*, 17 (2019), pp. 1737–1755.
- [18] P. FIFE, *Some nonclassical trends in parabolic and parabolic-like evolutions*, *Trends in nonlinear analysis*, (2003), pp. 153–191.
- [19] G. GILBOA AND S. OSHER, *Nonlocal linear image regularization and supervised segmentation*, *Multiscale Modeling & Simulation*, 6 (2007), pp. 595–630.
- [20] G. GILBOA AND S. OSHER, *Nonlocal operators with applications to image processing*, *Multiscale Modeling & Simulation*, 7 (2009), pp. 1005–1028.
- [21] Y. D. HA AND F. BOBARU, *Characteristics of dynamic brittle fracture captured with peridynamics*, *Engineering Fracture Mechanics*, 78 (2011), pp. 1156–1168.
- [22] R. B. LEHOUCQ AND S. T. ROWE, *A radial basis function galerkin method for inhomogeneous nonlocal diffusion*, *Computer Methods in Applied Mechanics and Engineering*, 299 (2016), pp. 366–380.
- [23] Y. LENG, X. TIAN, L. DEMKOWICZ, H. GOMEZ, AND J. T. FOSTER, *A petrov-galerkin method for nonlocal convection-dominated diffusion problems*, *arXiv preprint arXiv:2107.07080*, (2021).
- [24] Y. LENG, X. TIAN, N. TRASK, AND J. T. FOSTER, *Asymptotically compatible reproducing kernel collocation and meshfree integration for nonlocal diffusion*, *SIAM Journal on Numerical Analysis*, 59 (2021), pp. 88–118.
- [25] Y. LENG, X. TIAN, N. A. TRASK, AND J. T. FOSTER, *Asymptotically compatible reproducing kernel collocation and meshfree integration for the peridynamic navier equation*, *Computer Methods in Applied Mechanics and Engineering*, 370 (2020), p. 113264.
- [26] D. J. LITTLEWOOD, *Simulation of dynamic fracture using peridynamics, finite element modeling, and contact*, in *ASME International Mechanical Engineering Congress and Exposition*, vol. 44465, 2010, pp. 209–217.
- [27] Y. LOU, X. ZHANG, S. OSHER, AND A. BERTOZZI, *Image recovery via nonlocal operators*, *Journal*

- of Scientific Computing, 42 (2010), pp. 185–197.
- [28] M. M. MEERSCHAERT AND A. SIKORSKII, *Stochastic models for fractional calculus*, de Gruyter, 2019.
- [29] T. MENGESHA, *Nonlocal korn-type characterization of sobolev vector fields*, Communications in Contemporary Mathematics, 14 (2012), p. 1250028.
- [30] T. MENGESHA AND Q. DU, *The bond-based peridynamic system with dirichlet-type volume constraint*, Proceedings of the Royal Society of Edinburgh Section A: Mathematics, 144 (2014), pp. 161–186.
- [31] T. MENGESHA AND Q. DU, *On the variational limit of a class of nonlocal functionals related to peridynamics*, Nonlinearity, 28 (2015), p. 3999.
- [32] R. METZLER AND J. KLAFTER, *The random walk’s guide to anomalous diffusion: a fractional dynamics approach*, Physics Reports, 339 (2000), pp. 1–77.
- [33] M. L. PARKS, P. SELESON, S. J. PLIMPTON, R. B. LEHOUCQ, AND S. A. SILLING, *Peridynamics with lammps: A user guide*, Sandia National Laboratory Report, SAND2008-0135, Albuquerque, New Mexico, (2008).
- [34] A. C. PONCE, *An estimate in the spirit of poincaré’s inequality*, Journal of the European Mathematical Society, 6 (2004), pp. 1–15.
- [35] P. SELESON AND M. PARKS, *On the role of the influence function in the peridynamic theory*, International Journal for Multiscale Computational Engineering, 9 (2011).
- [36] S. A. SILLING, *Reformulation of elasticity theory for discontinuities and long-range forces*, Journal of the Mechanics and Physics of Solids, 48 (2000), pp. 175–209.
- [37] S. A. SILLING AND E. ASKARI, *A meshfree method based on the peridynamic model of solid mechanics*, Computers & Structures, 83 (2005), pp. 1526–1535.
- [38] Y. TAO, X. TIAN, AND Q. DU, *Nonlocal diffusion and peridynamic models with Neumann type constraints and their numerical approximations*, Applied Mathematics and Computation, 305 (2017), pp. 282–298.
- [39] H. TIAN, L. JU, AND Q. DU, *A conservative nonlocal convection–diffusion model and asymptotically compatible finite difference discretization*, Computer Methods in Applied Mechanics and Engineering, 320 (2017), pp. 46–67.
- [40] H. TIAN, H. WANG, AND W. WANG, *An efficient collocation method for a non-local diffusion model*, International Journal of Numerical Analysis & Modeling, 10 (2013).
- [41] X. TIAN AND Q. DU, *Analysis and comparison of different approximations to nonlocal diffusion and linear peridynamic equations*, SIAM Journal on Numerical Analysis, 51 (2013), pp. 3458–3482.
- [42] X. TIAN AND Q. DU, *Asymptotically compatible schemes and applications to robust discretization of nonlocal models*, SIAM Journal on Numerical Analysis, 52 (2014), pp. 1641–1665.
- [43] X. TIAN AND Q. DU, *Asymptotically compatible schemes for robust discretization of parametrized problems with applications to nonlocal models*, SIAM Review, 62 (2020), pp. 199–227.
- [44] N. TRASK, H. YOU, Y. YU, AND M. L. PARKS, *An asymptotically compatible meshfree quadrature rule for nonlocal problems with applications to peridynamics*, Computer Methods in Applied Mechanics and Engineering, 343 (2019), pp. 151–165.
- [45] C. VOLLMANN, *Nonlocal models with truncated interaction kernels-analysis, finite element methods and shape optimization*, PhD thesis, University of Trier, 2019.
- [46] C. WANG AND H. WANG, *A fast collocation method for a variable-coefficient nonlocal diffusion model*, Journal of Computational Physics, 330 (2017), pp. 114–126.
- [47] J. Z. YANG, X. YIN, AND J. ZHANG, *On uniform second-order nonlocal approximations to diffusion and subdiffusion equations with nonlocal effect parameter*, Communications in Mathematical Sciences, Accepted (***) , p. ***.
- [48] H. YOU, X. LU, N. TASK, AND Y. YU, *An asymptotically compatible approach for neumann-type boundary condition on nonlocal problems*, ESAIM: Mathematical Modelling and Numerical Analysis, 54 (2020), pp. 1373–1413.
- [49] X. ZHANG, M. GUNZBURGER, AND L. JU, *Quadrature rules for finite element approximations of 1d nonlocal problems*, Journal of Computational Physics, 310 (2016), pp. 213–236.
- [50] X. ZHANG, J. WU, AND L. JU, *An accurate and asymptotically compatible collocation scheme for nonlocal diffusion problems*, Applied Numerical Mathematics, 133 (2018), pp. 52–68.
- [51] G. ZHENG, J. WANG, G. SHEN, Y. XIA, AND W. LI, *A new quadrature algorithm consisting of volume and integral domain corrections for two-dimensional peridynamic models*, International Journal of Fracture, (2021), pp. 1–16.